Materials Letters 201 (2017) 181–184

Contents lists available at ScienceDirect

Materials Letters

journal homepage: www.elsevier.com/locate/mlblue

Novel controlled synthesis of nanoporous carbon nanorods from resorcinol-formaldehyde xerogels

Ahmed Awadallah-F [1], Shaheen A. Al-Muhtaseb *

Department of Chemical Engineering, Qatar University, PO Box 2713, Doha, Qatar

ARTICLE INFO

Article history:
Received 2 April 2017
Received in revised form 27 April 2017
Accepted 2 May 2017
Available online 4 May 2017

Keywords:
Carbon materials
Carbon nanorods
Sol-gel preparation
Porous materials
Resorcinols
Formaldehydes

ABSTRACT

A novel approach is discovered to produce carbon nanorods (CNRs) from resorcinol-formaldehyde xerogels. The structure and morphology of CNRs are characterized by pore size analysis, nano-scanning electron microscopy, elemental analyses and Raman spectra, FTIR spectroscopy. CNRs exhibited diameter ranges from 262 to 327 nm and lengths of up to several microns. The growth rate of CNRs depends fundamentally on the gelation temperature. CNRs' structures exhibits nanopores with average pore sizes of 2.39 and ~1.64 nm for CNRs produced from xerogels glated at 70 and 85 °C, respectively. It is anticipated for CNRs to open new gates for advanced nano-device applications.

1. Introduction

Since the discovery of carbon nanotubes (CNTs) [1], much attention has been focused on one dimensional (1D) nanostructures like nanotubes and nanowires because of their fundamental importance and their anticipated wide range of applications in nano-devices that would enhance human's life [2]. CNRs have two advantages over CNTs. Firstly, the properties of CNRs can be controlled more precisely by either manipulating the synthesis conditions or using a doping techniques. Secondly, the native oxide layer that can be formed on the outside of CNRs allows the application of a broad range of already well developed functionalization and blocking chemistries [3]. Although numerous techniques have been developed for the fabrication of CNTs and 1D nanomaterials, the exploration of new methods and controllable synthesis of 1D nanostructures under ambient conditions is still an interesting and challenging topic [1,4–6].

Generally, such kind of nanostructures could be prepared by two methods. The first method is by a "bottom-up" approach, where the self-assembly of small sized structures build into larger structures. The other method is a by "top-down" approach, where large structures are reduced down into smaller sizes to produce nanoscale structures [7]. Several methods were developed for the fabrication of nano-rod or nano-wire arrays, including catalytic growth, template [8], Langmuir Blodgett method and electrospinning [9]. Nonetheless, all these methods are not practical in mass production and are expensive.

The motivation for this study comes from the difficult challenges of the above-mentioned synthesis processes to produce CNRs. In this work [10], CNRs are prepared from the polymerization of resorcinol and formaldehyde in presence of sodium carbonate, followed by atmospheric drying, carbonization and activation [11]. This novel method of synthesizing CNRs can provide a large scale and controllable route to provide a low cost supply for raw nanowires and their corresponding nano-devices.

2. Materials and methods

Resorcinol (99.98%, Alfa Aesar), formaldehyde (37 wt%, Aldrich), sodium carbonate (anhydrous, Fisher) and acetone (99.6%, Fisher) were used as received. Other reagents are analytical grade. Resorcinol–formaldehyde (RF) xerogels have been prepared with a resorcinol-to-formaldehyde molar ratio of 0.3; a resorcinol-to-water molar ratio of 0.05; a resorcinol-to-catalyst molar ratio of 50; and an initial solution pH of 7. RF solutions were poured into polypropylene vials, sealed and placed in an oven 7 days [12]. Oven temperatures were set at 70 °C and 85 °C for the consequent activated carbons denoted as RF-ACX-1 and RF-ACX-2, respectively. Other details of xerogels' synthesis, carbonization and activation,

* Corresponding author.
E-mail address: s.almuhtaseb@qu.edu.qa (S.A. Al-Muhtaseb).
[1] Dr. A. Awadallah-F is on leave the Radiation Research of Polymer Department, National Centre for Radiation Research and Technology, Atomic Energy Authority, P.O. Box 29, Nasr City, Cairo, Egypt.

http://dx.doi.org/10.1016/j.matlet.2017.05.021
0167-577X/

characterization, and adsorption/desorption isotherms are found in the Supporting Information Data File.

3. Results and discussion

NanoSEM morphologies of RF-ACX-1 and RF-ACX-2 are shown in Fig. 1 with different magnifications. Morphologies indicate that both samples formed whisker nanowires in the shape of nanorods. The nanorods of RF-ACX-1 and RF-ACX-2 differ in their size distributions and nanoparticle levels. The CNRs in RF-ACX-1 appear in Fig. 1c and e as bundles of sticks, whereas the nanorods of RF-ACX-2 appear in Fig. 1d and f as scattered entities. This hints that the growth rate of CNRs depends on the gelation temperature. A high temperature of 85 °C may lead to a more crosslinked chains than those at a low temperature of 70 °C, which could make CNRs more rigid and appearing as compact rods when gelated at 85 °C or fragile rods when gelated at 70 °C after carbonization and activation. The reaction mechanism of synthesis was found in elsewhere [13]. The average nanorod diameter of RF-ACX-1 (~262 nm) is lower than that of RF-ACX-2 (~327 nm). This is attributed to the corresponding differences in their precursors' gelation temperatures. CNRs produced from precursors gelated at low temperatures exhibited clear patterns of nanoparticles, whereas those corresponding to high temperatures were relatively smooth. NanoSEM micrographs of both appear as long cylindrical products with several microns in length.

Fig. 2 shows the pore size distribution (PSD) for RF-ACX-1 and RF-ACX-2. It was observed that a majority (~81% and 85% for RF-ACX-1 and RF-ACX-2, respectively) of pores exhibited incremental surface areas located in microporous region (≤2 nm). Relatively small percentages (~19% and ~15% for RF-ACX-1 and RF-ACX-2, respectively) were in mesoporous region (>2 to 50 nm) and a

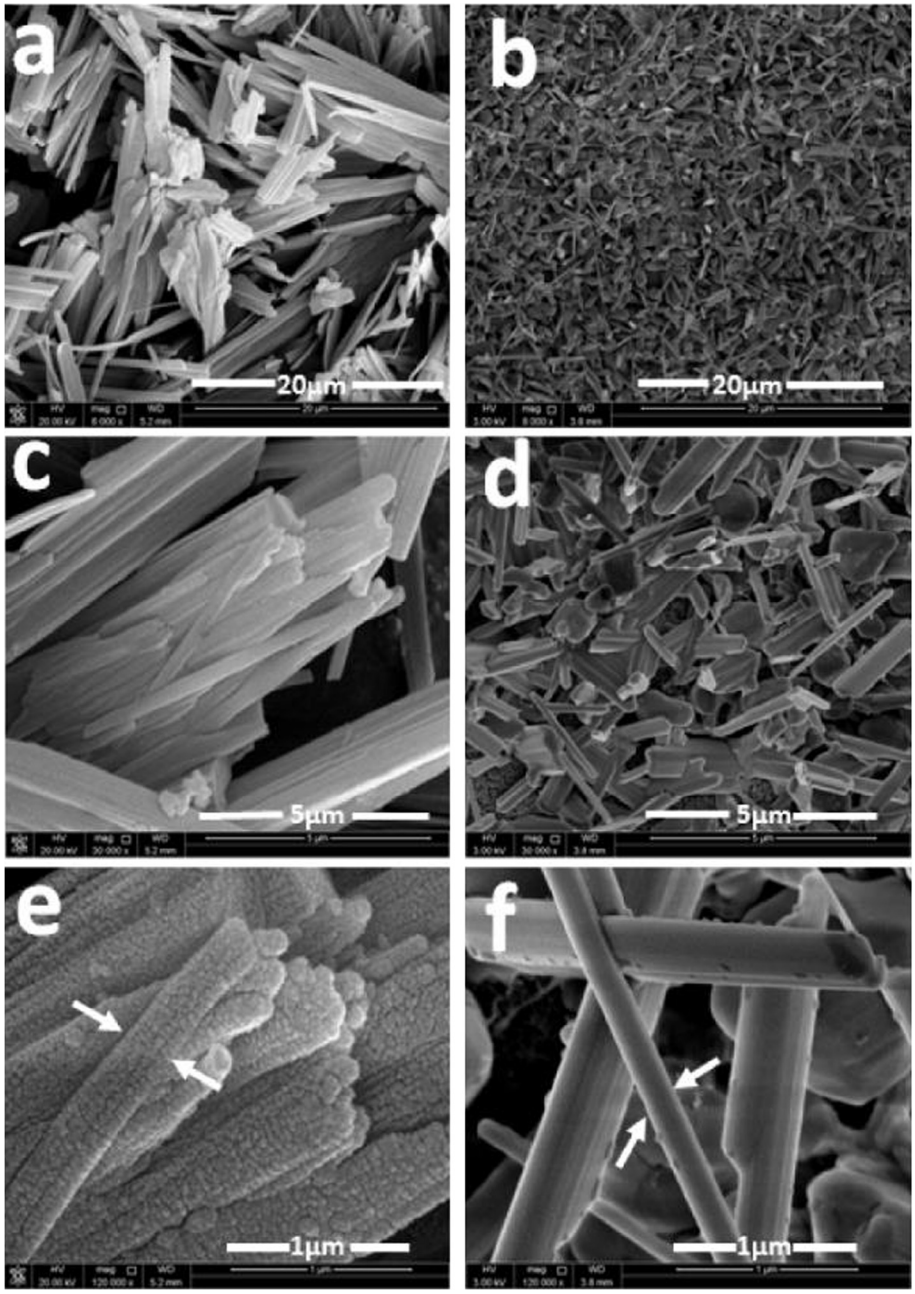

Fig. 1. Morphologies of RF-ACX-1 (a, c, e) and RF-ACX-2 (b, d, f) at different magnifications.

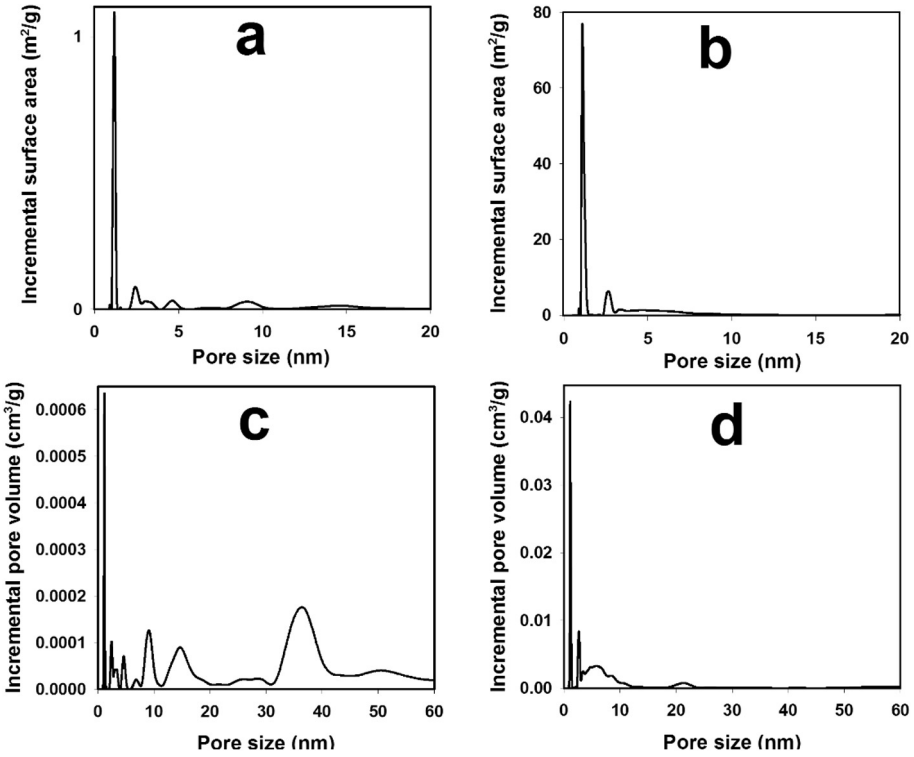

Fig. 2. PSD in terms of incremental surface area (a, b) and incremental pore volume (c, d) for RF-ACX-1 (a, c) and RF-ACX-2 (b, d).

Table 1
Pore characteristics[a] and elemental compositions[b] of RF-ACX-1 and RF-ACX-2.

Characteristics	Sample	
	RF-ACX-1	RF-ACX-2
Pore characteristics		
Average surface pore size (nm)	2.4	1.7
Total area (m^2/g)	2.5	179
Micropore area (%)	81	85
Mesopore area (%)	19	15
Macropore area (%)	0.20	0.03
Total pore volume (cm^3/g)	3×10^{-3}	0.15
Micropore volume (%)	39	60
Mesopore volume (%)	56	38
Macropore volume (%)	5	1.7
N_2 adsorption capacity at saturation (mmol/g)	0.209	5
Elemental compositions		
Carbon (wt%)	90	86
Oxygen + Sodium (wt%)	10	14

[a] Determined from DFT of adsorption/desorption isotherms of N_2 at 77 K (Fig. S1, Supporting Information Data File).
[b] Determined by elemental microanalysis (C, H, N, and S) and by balance difference (O + Na).

minority (~0.2% and ~0.03% for RF-ACX-1 and RF-ACX-2, respectively) were in macroporous region (>50 nm). Fig. 2c and d expose the PSDs for RF-ACX-1 and RF-ACX-2, respectively, in terms of incremental pore volumes. It was illustrated from Fig. 2c that the RF-ACX-1 exhibited mostly microporous volume distribution with a notable presence of mesoprores. The microporous pore volume region was characterized by sharp peaks with ~39%, while mesoporous pore volume region was characterized by multiple different peaks ~56% of total pore volume, and a macroporous volume portion of ~5%. The PSD of RF-ACX-2 (Fig. 2d) showed that microporous pore volume also appeared as a sharp peak at a pore size (≤2 nm) at ~60% of total volume, while mesopores and macropores constituted were ~39% and ~1.7%, of total pore volume, respectively. The bigger extent of mesopores in RF-ACX-1 may be attributed to the collection of voids among CNRs due to their prominent bundled patterns, which is less evident in RF-ACX-2 (Fig. 1). Table 1 summarizes pore characteristics and elemental analyses of RF-ACX-1 and RF-ACX-2 CNRs. The pore size characteristics indicate to the differences in pore structures of two samples. This difference is due to the gelation temperature.

The chemical compositions of two samples are somewhat similar with small differences. The variation of synthesis temperature reflects significantly on physical changes (Table 1).

Fig. 3a shows FTIR spectra of RF-ACX-1(a) and RF-ACX-2(b), respectively. It was observed that the two spectra are similar. Therefore, the chemical structures of both CNRs are identical. The peaks appearing at 1062 and 1726 cm^{-1} indicate to C–O and C═O, respectively.

Raman spectra of RF-ACX-1 and RF-ACX-2 (Fig. 3b) expose that the spectrum of RF-ACX-1 has only two peaks at 1334 and 1584 cm^{-1}), whereas RF-ACX-2 has three peaks at 1334, 1584 and 840 cm^{-1}. It is observed that the two main bands at ~1584 cm^{-1} (G-band) and at ~1334 cm^{-1} (D-band) are assigned, respectively, to in-plane vibration of the C–C bond for typical graphite-like materials and the presence of disorder in carbon systems [12,14]. Hence, the ratio of D-band intensity to G-band intensity (I_D/I_G) is an indication of defects or graphitic order [15]. The value of I_D/I_G for MWCNTs, graphite, graphite oxide and reduced graphite oxide are 0.94, 0.7, 1.03 and 0.93, respectively [16]. The intensity ratio (I_D/I_G) for both of RF-ACX-1 and RF-ACX-2 is similar at 0.87. Therefore, CNRs are more closely characterized to graphitic order.

4. Conclusions

A recipe was discovered to synthesize activated carbons from resorcinol-formaldehyde xerogels in a form of carbon nanorods

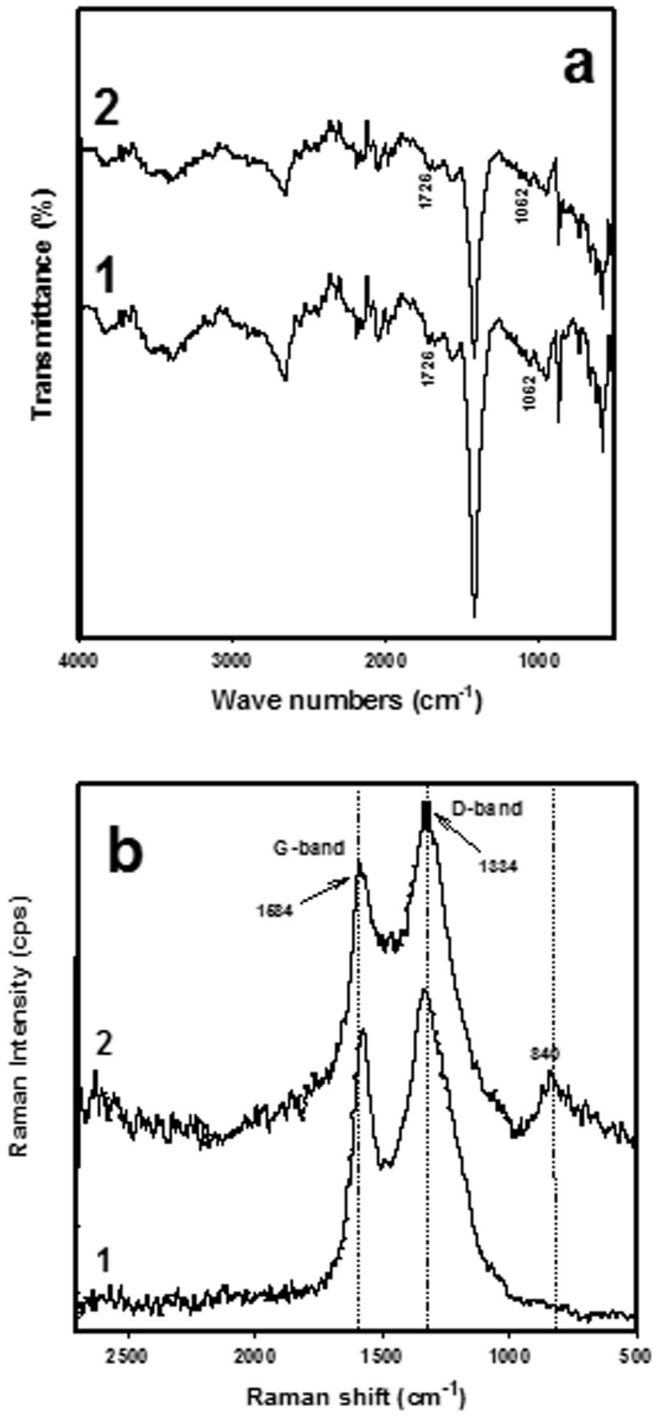

Fig. 3. (a) FTIR spectra of RF-ACX-1(curve) and RF-ACX-2(curve 2), respectively and (b) Raman spectra of RF-ACX-1 and RF-ACX-2 (curves 1 and 2, respectively).

(CNRs). The CNRs were characterized by different techniques. The structures exhibited nanorods/nanowires that can have lengths of several microns. The nanowire growth depended on the synthesis gelation temperature of the precursor xerogel. CNRs gelated at low temperatures exhibited clear patterns of nanoparticles, whereas those corresponding to high gelation temperatures were relatively smooth. Furthermore, CNRs corresponding to xerogels gelated at low temperatures appeared as bundles, while those corresponding to higher temperature appeared in a more separated form. This method opens a new gate of synthesis nanotechnology with easy procedures and inexpensive techniques. Overall, the dimensional geometry of carbon nanowires can be useful in many nano applications.

Acknowledgments

This publication was made possible by the support of the NPRP awards [NPRP 08-014-2-003 and NPRP-8-001-2-001] from the Qatar National Research Fund (a member of The Qatar Foundation). The statements made herein are solely the responsibility of the authors. Technical support from the Department of Chemical Engineering and the Central Laboratory Unit at Qatar University is also acknowledged.

Appendix A. Supplementary data

Supplementary data associated with this article can be found, in the online version, at http://dx.doi.org/10.1016/j.matlet.2017.05.021.

References

[1] S. Iijima, Helical microtubules of graphitic carbon, Nature 354 (1991) 56–58.
[2] W.B. Choi, D.S. Chung, J.H. Kang, H.Y. Kim, Y.M. Jin, I.T. Han, Y.H. Lee, J.E. Jung, N.S. Lee, G.S. Park, J.M. Kim, Fully sealed, high-brightness carbon-nanotube field-emission display, Appl. Phys. Lett. 75 (1999) 3129–3131.
[3] U. Yogeswaran, S.-M. Chen, A Review on the electrochemical sensors and biosensors composed of nanowires as sensing material, Sensors 8 (2008) 290–313.
[4] M. Endo, K. Takeuchi, S. Igarashi, K. Kobori, M. Shiraishi, H.W. Kroto, The production and structure of pyrolytic carbon nanotubes (PCNTs), J. Phys. Chem. Solids 54 (1993) 1841–1848.
[5] D.L. Baptista, F.C. Zawislak, Hard and sp2-rich amorphous carbon structure formed by ion beam irradiation of fullerene, a-C and polymeric a-C: H films, Diamond Relat. Mater. 1 (2004) 1791–1801.
[6] S. Ahmed, A. Aitani, F. Rahman, A. Al-Dawood, F. Al-Muhaish, Decomposition of hydrocarbons to hydrogen and carbon, Appl. Catal. A 359 (2009) 1–24.
[7] A. Vaseashta, D. Dimova-Malinovska, Nanostructured and nanoscale devices, sensors and detectors, Sci. Tech. Adv. Mat. 6 (2005) 312–318.
[8] S.J. Limmer, G.Z. Cao, Sol–gel electrophoretic deposition for the growth of oxide nanorods, Adv. Mater. 15 (2003) 427–431.
[9] X.D. Wang, C.J. Summers, Z.L. Wang, Large-scale hexagonal-patterned growth of aligned ZnO nanorods for nano-optoelectronics and nanosensor arrays, Nano Lett. 4 (2004) 423–426.
[10] A. Awadallah-F, S.A. Al-Muhtaseb, Method of synthesising carbon nanorods and nanowires, U.S. Patent No. 9,598,287 B2, 2017.
[11] Z. Xu, J. Wang, Z. Hu, R. Geng, L. Gan, Structure evolutions and high electrochemical performances of carbon aerogels prepared from the pyrolysis of phenolic resin gels containing ZnCl2, Electrochim. Acta 231 (2017) 601–608.
[12] A. Awadallah-F, S.A. Al-Muhtaseb, Nanofeatures of resorcinol–formaldehyde carbon microspheres, Mater. Lett. 87 (2012) 31–34.
[13] A. Awadallah-F, A.M. Elkhatat, S.A. Al-Muhtaseb, Impact of synthesis conditions on meso-and macropore structures of resorcinol–formaldehyde xerogels, J. Mater. Sci. 46 (2011) 7760–7769.
[14] K. Zhang, Y. Zhang, S. Wang, Sci. Rep. 3 (2013), http://dx.doi.org/10.1038/srep03448 3448.
[15] S.L.H. Rebelo, A. Guedes, M.E. Szefczyk, A.M. Pereira, J.P. Araújo, C. Freire, Progress in the Raman spectra analysis of covalently functionalized multiwalled carbon nanotubes: unraveling disorder in graphitic materials, Phys. Chem. Chem. Phys. 18 (2016) 12784–12796.
[16] M. Liu, X. Ma, L. Gan, Z. Xu, D. Zhu, L. Chen, A facile synthesis of a novel mesoporous Ge@C sphere anode with stable and high capacity for lithium ion batteries, J. Mater. Chem. A 2 (2014) 17107–17114.